

Article

Not peer-reviewed version

Bonding with a UV Ozone Cleaner – A Practical Guide to Prepare a Microfluidic Chip

[Mirjam P.M. Poschmann](#)*, [Lucas Holtorf](#), [Igor Titov](#), [Martina Gerken](#)*

Posted Date: 31 March 2026

doi: 10.20944/preprints202603.2487.v1

Keywords: microfluidics; bonding; UV ozone treatment



Preprints.org is a free multidisciplinary platform providing preprint service that is dedicated to making early versions of research outputs permanently available and citable. Preprints posted at Preprints.org appear in Web of Science, Crossref, Google Scholar, Scilit, Europe PMC.

Copyright: This open access article is published under a [Creative Commons CC BY 4.0 license](#), which permit the free download, distribution, and reuse, provided that the author and preprint are cited in any reuse.

Disclaimer/Publisher's Note: The statements, opinions, and data contained in all publications are solely those of the individual author(s) and contributor(s) and not of MDPI and/or the editor(s). MDPI and/or the editor(s) disclaim responsibility for any injury to people or property resulting from any ideas, methods, instructions, or products referred to in the content.

Article

Bonding with a UV Ozone Cleaner – A Practical Guide to Prepare a Microfluidic Chip

Mirjam P. M. Poschmann ^{1,*}, Lucas Holtorf ¹, Igor Titov ¹ and Martina Gerken ^{1,2,*}

¹ Integrated Systems and Photonics, Faculty of Engineering, Kiel University, Germany, Kaiserstraße 2, 24143 Kiel

² Kiel Nano, Surface and Interface Sciences (KiNSIS)

* Correspondence: mip@tf.uni-kiel.de (M.P.M.P.); mge@tf.uni-kiel.de (M.G.)

Abstract

This study describes a procedure for preparing microfluidic chips made from polydimethylsiloxane (PDMS). It uses a UV ozone cleaner for surface activation instead of the more common oxygen plasma treatment. Although this process has some limitations compared to oxygen plasma bonding, it can be used when a low-cost procedure for a small number of microfluidic chips is required or when an oxygen plasma etcher is unavailable. The challenges of this process arise from the slight hardening of the PDMS surface when it is activated for 70 minutes, which is necessary for reliable bonding. It is demonstrated that damage resulting from this hardening in conjunction with careless handling of the microfluidic chip is mitigated by incorporating predetermined break structures and using tubes with an outer diameter that is smaller than the inlets. Additionally, pre-polymerized PDMS glue and PDMS seals are suggested to ensure that the tubes are properly sealed. To demonstrate the concept, two microfluidic structures were prepared and tested, achieving flow rates of at least 170 $\mu\text{L}/\text{min}$ at ± 180 mbar. Bonding remains stable up to a pressure of approximately 0.5 bar.

Keywords: microfluidics; bonding; UV ozone treatment

1. Introduction

In recent decades, microfluidic devices have become a field of high interest due to their variability and adaptability, which ensures their use in a wide range of biological and chemical point-of-care analysis devices [1–5]. So-called 'lab-on-a-chip' devices enable test reagents to be combined within microchannel systems for various purposes, such as mixing, separating, filtering, carrying out chemical reactions and taking measurements, when combined with additional measurement compounds [6–10]. These systems are operated using, e.g., micro-pumps and valves [2,11,12]. The chips are made from various polymers, such as poly(methyl methacrylate), polystyrene, poly(dimethyl siloxane) (PDMS), as well as less common polymers for special applications. Production methods include injection molding, cutting, 3D printing and lithography [2,13–15]. These methods are used to create layers with one-site open channel systems that are closed by bonding them to a substrate. Bonding is therefore a central process step in microfluidic chip fabrication, and multiple different methods have been described, e.g. applying a tape, or glue, using a chemical or physical surface modifications, or hot embossing [16–18].

The use of PDMS is one of multiple options and especially common in research laboratories and during the prototyping phase due to its optical transparency and fast preparation and integration of the chips [19,20]. Small batches of these chips are often produced using photolithography and soft lithography processes, but also other molds are used. In this process, a one-side open channel system is created in a PDMS layer using a wafer master as a mold. The PDMS layer is then sealed by bonding it to a substrate, such as glass or polymers [20–22]. This bonding is most often achieved by bringing the two layers into contact after they have been activated in an oxygen plasma, as this is usually a highly reliable process [23]. However, we observed some challenges when working with an SI 100 by

Sentech, as it is an older instrument used for multiple processes. We had to adapt our bonding protocol several times when issues occurred, such as smaller or larger leakages, different pressure in the gas supply line, hardware changes after maintenance work was performed, or contamination of the chamber by other processes. These problems resulted in inconsistent bonding, so alternatives were tested simultaneously. One option is to use a PDMS/toluene mixture or a prepolymerized PMDS [24,25]. However, both methods result in low bonding strength. Additionally, the glue partially or fully blocks small channels, meaning it cannot be used for channels measuring 200 μm x 200 μm or smaller. Another possibility is a UV ozone treatment (UVO), which is a well established method for substrate cleaning and surface functionalization [26]. Successful bonding was achieved using UV or UVO treatment alongside thermal bonding at temperatures 5-10 $^{\circ}\text{C}$ lower than the individual glass transition temperatures T_g or the Vicat softening point T_v for poly(methylmethacrylate) ($T_g = 98^{\circ}\text{C}$) [27,28], cyclic olefin copolymer ($T_g = 105^{\circ}\text{C}$) [28], polystyrene ($T_v = 93^{\circ}\text{C}$) and cyclic polyolefine ($T_g = 70^{\circ}\text{C}$) [29].

During UVO treatment of PDMS, oxygen dissociates at a wavelength of 184.9 nm, while ozone dissociates at 253.7 nm. The latter wavelength is absorbed by hydrocarbons, leading to their oxidation by reactive oxygen species [30]. This process involves removing the methyl groups from the PDMS surface and the bulk material close to the surface and forming a thin, glass-like, amorphous SiO_2 layer. The thickness of this layer depends on the treatment time and lamp intensity. The treatment results in long-lasting hydrophilic behavior, which could be useful for certain applications [30,31]. However, the treatment results in slight hardening of the surface. BERDICHEVSKY et al. [31] describe cracks forming when the device's temperature exceeds 100 $^{\circ}\text{C}$ and the treatment time exceeds 30 minutes. Additionally, they observed a permanently reduced contact angle after 2h treatment times. To bond the surface, the researchers in that study applied an additional thin PDMS film and used oxygen plasma bonding and not UVO bonding.

YOUSUFF et al. [32] compared the bonding strength of PDMS@glass and PDMS@PDMS samples bonded using UVO and oxygen plasma treatments. The bonding strength with UVO was higher in the case of PDMS@glass (314 \pm 20 kPa) and lower in the case of PDMS@PDMS (95 \pm 20 kPa) compared to oxygen plasma treatment (279 \pm 20 kPa and 180 \pm 20 kPa, respectively). The same observation was made regarding PDMS@PDMS bonding by CHEN et al. [33] (0.78 \pm 0.08 MPa vs. 2.34 \pm 0.27 MPa). In some other studies, researchers utilize UVO bonding to prepare microfluidic systems and we summarized the information concerning the bonding in the SI in Table S1. Treatment times ranging between 3 - 40 min and various aftertreatments at elevated temperatures are used. However, the focus of all these studies is on the investigated devices rather than on the UVO bonding process itself. There is very little information on the UVO bonding, so it is difficult to identify the reasons for the different conditions. We were unable to reproduce the results using our UV ozone cleaner (L2002A3-EU model by Ossila Ltd), possibly due to differences in the instruments, geometries, intensities or other parameters.

To the best of our knowledge, no study has discussed the challenges, limitations and reproducibility of UVO bonding for microfluidic chip preparation, which is important for its further deployment. In this study, we present a method for preparing PDMS-based microfluidic chips with our UV ozone cleaner by Ossila. We observed issues arising from the hardening of the PDMS surface and explored ways to address the most important factors in preparing a microfluidic chip: These were the optimization of bonding conditions, the mechanical stability in the context of a lower bonding strength and the leakage prevention (see Figure 1). Finally, we demonstrate the working range by preparing two microfluidic chips and showing their functionality and limitations.

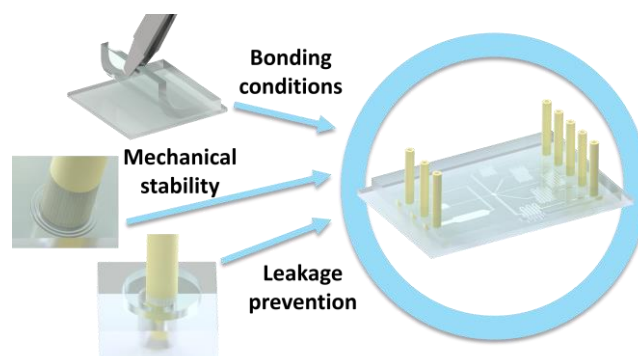


Figure 1. Schematic overview of the most important factors for creating a microfluidic chip that are discussed within this study.

2. Materials and Methods

Si-wafer 4P0/5-10/525±20/SSP/TTV<5 (Sigert Wafer), GM1075 photoresist (Gersteltec), 1-Methoxy-2-propylacetat PGMEA (Carl Roth), Polydimethylsiloxane PDMS (Sylgard™ 184 and Curing Agent by Dow Corning), polished float glass (Präzisions Glas & Optik GmbH), spin coater Opti Spin ST22P (ATMae GmbH), mask aligner MA6/BA6 (Süss MicroTec Lithography GmbH), Plasma etcher SI 100 (Sentech), UV Ozone Cleaner with emission at 185 and 254 nm and with an intensity of 15 mW/cm² at 185 nm (Ossila), Confocal microscope VK-X260-K (Keyence), pressure sensor ABPDRRV015PDAA5 (Honeywell International Inc), peristaltic pump RP-QIICP5S-P18A-DC3VS (Takasago Electric, Inc.) actuated with an electronic board and a Raspberry PI as described before [34] are used.

2.1. Photolithography

Prior to the usage the wafer was cleaned 5 min in acetone, isopropanol and water each in an ultrasonic bath and dehydrated for 5 min on a hotplate at 150 °C. The surface activation was performed in an oxygen plasma etcher for 6 min at 0.3 mbar and 300 W. Afterwards GM1075 was spin coated on the wafer using in a first step a ramp of 100 rpm/s up to 1900 rpm and holding that for 110 s and a second step in which spinning was increased for 1 s to 2300 rpm with 400 rpm/s. Afterwards the wafer was placed on a horizontally levelled hotplate at 40 °C for 30 min. Then a heat ramp of 4 °C/min was used to reach 120 °C and we held that temperature for 2 min. Afterwards the wafer was cooled down to room temperature and exposed to UV light (I-line) with 200 mJ/cm². The post exposure bake was performed for 2 min at 65 °C and 25 min at 95 °C. After one day of waiting time, the wafer was developed in PGMEA for 4.75 min. The structure thickness was confirmed with a confocal microscope.

2.2. Soft Lithography

A PDMS mixture with a 10:1 Sylgard™ 184:Curing Agent ratio was prepared in quantities of 20 or 30 g for PDMS layers with thicknesses of 2 mm and 3 mm, respectively. This mixture was then thoroughly mixed and degassed in a desiccator. The wafer master was placed in an aluminum foil mold, into which the PDMS mixture was poured and degassed again. The PDMS was then cured for 20 minutes at 130 °C on a hot plate. Afterwards, it was peeled off the wafer and cut into pieces. In case of the samples for the bonding optimization a blank wafer was used and the created PDMS layer was cut into 1 × 1 cm pieces.

2.3. Optimization of Bonding Conditions

PDMS sheets, 2–3 mm thick, were cut into 1 cm × 1 cm pieces. These were cleaned in an ultrasonic bath with acetone for 1 min each, then dried on a hot plate at 130 °C for five minutes. The glass pieces

(2.5 cm × 2.5 cm) were cleaned in an ultrasonic bath with acetone and IPA for 5 min, and then dried on a hot plate at 130 °C for 15 min. Most times, seven different positions were tested in the measurement to average out mistakes and confirm a homogeneous activation within the chamber (see SI Figure S1). If the samples were to be treated equally, activation in the Ozon Cleaner was performed in parallel for the same amount of time. If different times were used, the glass was usually treated for the difference in time between the two samples. After this, the two samples were activated together for the remaining time. The samples were pressed together within the first minute after activation using only slight pressure (Figure 2). A post-treatment at 80 °C was then performed for 1h.

UVO treatments lasting between 10 and 90 minutes were tested and the positions of the samples were noted to determine whether the treatment was homogeneous across the entire chamber. After 20–24 hours, the samples were peeled off to test the bonding.

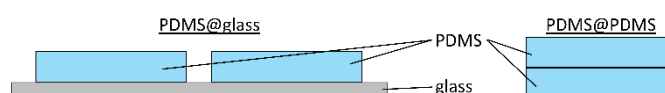


Figure 2. Schematic illustration of the bonding optimization samples.

2.4. Peel Test

There are several methods to determine the bonding strength [23]. We selected a manual peel test for the optimization of the bonding conditions because it does not require any special sample preparation or equipment and is easily adaptable to different sample sizes. Our primary interest lay in creating a strong enough bond to prevent delamination of the layers. In this instance, values obtained using more precise methods would only indicate the breaking point of the PDMS layers and would not provide accurate bonding strength values.

2.5. Predetermined Breaking Structures

To investigate the mechanical stability of inlets and outlets, the predetermined breaking structures were designed. A master wafer was prepared, and 2 mm thick PDMS layers were prepared as described above. These layers were then bonded using a 70 min UVO treatment. Tubes of two different sizes (i.e., 1.0 and 1.6 mm outer diameter) were inserted, and the influence of insertion and slight and strong movement was investigated using a confocal microscope. Figure 3 provides a schematic overview of the structures, while SI Figure S2 shows the more detailed structure as used for preparing the microfluidic chip.



Figure 3. Schematic design of the four predetermined breaking structures surrounding the inlets in comparison to the usual inlet (left). A more detailed version is given in SI Figure S3.

2.6. Sealing of the Tubes

If the PDMS does not seal the tubes automatically, for example if the hole is too big or the walls are no longer flexible enough, the tubes must be sealed properly to avoid leakage. This was achieved by gluing the tubes with PDMS and curing it at a high temperature. However, applying freshly prepared PDMS to the small gap between tube and layer is risky, as the PDMS can easily enter the gap and clog the microfluidic channel underneath. To prevent this, PDMS seals with an inner diameter of 1 or 1.5 mm, an outer diameter of 2, 3, 4 and 5 mm and a thickness of 0.1, 0.2 or 0.5 mm were prepared (Figure 4). A 1 cm tube with outer diameter of 1 or 1.6 mm was inserted in such a seal

and placed in an inlet of 1.5 or 2 mm size, respectively. Due to adhesion, the seal was able to slightly stick to the PDMS surface. Pre-polymerized PDMS glue was prepared by stirring an 8:1 PDMS mixture on a hot plate at 130 °C 9 times for 10 s each, until the viscosity was doubled. The glue was applied to the seal and fully cured on the hot plate at 130 °C. Afterwards, it was checked to see if the glue would have clogged the inlet or not. An overview of the process is given in SI Figure S5.

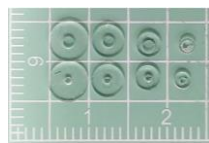


Figure 4. PDMS seals with 1.5 mm (top) and 1.0 mm inner diameter (bottom), 5, 4, 3 and 2 mm outer diameter (from left to right) and 0.5 mm thickness.

2.7. Leak and Burst Tests

Two microfluidic chips were prepared to demonstrate that functional microfluidic chips are produceable using a UVO treatment. A 2 mm thick unstructured PDMS substrate was used as the bottom layer. The structure of the top layer is shown in Figure 5. After punching, the layers were cleaned with acetone, dried at 130 °C and bonded following a 70 min UVO treatment. Afterwards, a 1 h post-treatment at 80 °C was performed. For **MF1**, the marked inlets were punched with a 1.5 mm biopsy punch. Tubes with an outer diameter of 1 mm and PDMS seals with an outer diameter of 4 mm and an inner diameter of 1 mm were used. For **MF2**, clogging of neighboring inlets might be a problem, when gluing the tubes one after another. Therefore, only the two outer and the middle inlets were punched with a 2 mm biopsy punch. Tubes of 1.6 mm outer diameter and PDMS seals with an outer diameter of 4 mm and an inner diameter of 1.5 mm were used. The glue was made by stirring an 8:1 PDMS mixture on a hot plate at 10-second intervals until the viscosity doubled (in total 110 s). The tubes were glued one after another while the chip was placed on a hot plate. Additionally, the glue was applied to the edge of the chips as a protection during the manual handling. The PDMS glue was then cured on a hot plate at 130 °C for 20 minutes.

For the leak and burst test, the inlets of the **MF1** or **MF2** chips were connected via Y-connectors and silicone tubes to a vessel containing blue ink colored water. The outlets were connected via Y-connectors to the tube with a pressure sensor and the peristaltic pump. The pump's flow rate was increased step by step, with the pumping direction always being changed to check the operation in a pressure- and in a vacuum-driven system within the same test. At the end of the test, all tubes were closed, while the pump ran to increase the pressure until a leakage occurred.

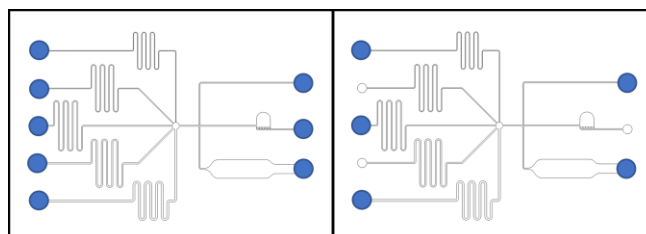


Figure 5. Structure of the microfluidic chips **MF1** (left) and **MF2** (right) with the punched inlets marked with blue cycles.

3. Results and Discussion

3.1. Optimization of the Bonding Process

The peel test results for all tested conditions are given in Tables 1 and 2, which show the results for glass@PDMS and PDMS@PDMS bonding, respectively. In the peel test, the samples were categorized as follows

- No bonding (colorless).
- Less than half of the area was bonded and/or the two layers could be separated with minimal force (yellow).
- More than half of the area was bonded and the two layers could only be separated by destroying the PDMS (blue).
- The whole area was bonded and the two layers could only be separated by destroying the PDMS (green).

Table 1. The PDMS@glass bonding conditions were evaluated in four categories: No bonding (colorless); Less than half of the area was bonded and the two layers could be separated with minimal force (yellow); More than half of the area was bonded and the two layers could only be separated by destroying the PDMS (blue); The whole area was bonded and the two layers could only be separated by destroying the PDMS (green).

Position	Activation time of glass / activation time of PDMS									
	min	min	min	min	min	min	min	min	min	min
top left	20/10	25/15	30/20	60/10	60/15	60/20	60/60	70/70	80/80	90/90
top right	20/10	25/15	30/20	60/10	60/15	60/20	60/60	70/70	80/80	90/90
middle left	20/10	25/15	30/20	60/10	60/15	60/20	60/60	70/70	80/80	90/90
middle	20/10	25/15	30/20	60/10	60/15	60/20	60/60	70/70	80/80	90/90
middle right	20/10	25/15	30/20	60/10	60/15	60/20	60/60	70/70	80/80	90/90
bottom left	20/10	25/15	30/20	60/10	60/15	60/20	60/60	70/70	80/80	90/90
bottom right	20/10	25/15	30/20	60/10	60/15	60/20	60/60	70/70	80/80	90/90

Table 2. The PDMS@PDMS bonding conditions and their evaluation as described before.

Position	Activation time of PDMS (same for both sides)									
	min	min	min	min	min	min	min	min	min	min
top left	10	15	20	30	40	50	60	70	-	-
top right	10	15	20	30	40	50	60	70	-	-
middle left	10	15	20	30	40	50	60	70	-	-
middle	10	15	20	30	40	50	60	70	80	90
middle right	10	15	20	30	40	50	60	70	-	-
bottom left	10	15	20	30	40	50	60	70	-	-
bottom right	10	15	20	30	40	50	60	70	-	-

Although bonding was exceptionally possible, no reproducible working conditions for bonding glass and PDMS were identified within the range of 10–90 min PDMS activation and 20–90 min glass substrate activation. However, bonding was possible in some cases. When taking into account the possibility of PDMS@glass bonding described in literature, this suggests that other parameters not included in this study have affected the outcome. Most likely this includes the temperature, the lamp intensity and the distance between the glass and the UV lamp. The latter is variably in some available UVO instruments and influences the intensity.

However, 70 min of treatment is sufficient for PDMS@PDMS bonding, and PDMS does not become damaged when left to activate for longer (i.e., for 80 or 90 min). For the samples marked in blue in the 70-minute test, only small spots on the edges of the PDMS pieces did not bond. Therefore, these conditions is useable to prepare microfluidic chips with a distance of 2–3 mm between structures and the edge.

Additionally, 110 μ m thick PDMS membranes were tested. However, weak bonding was observed in several tests when activation times of 10, 15 or 20 minutes were used. After 20 min of UVO treatment, the bonding was strong enough to prevent delamination when tubes were inserted

in only one out of four cases. Beyond 20 min of UVO treatment time the surface became rough, repellent and slightly opalescent. Moreover, it was observed that this surface change became more pronounced at higher temperatures within the range of 20–32 °C, as the instrument heated up during use within that range. This suggests that activation at temperatures below 20 °C might produce more consistent results, but this was not investigated in the context of this study. However, when PDMS is spin-coated onto a glass substrate and cured to form a layer of the same thickness as the membranes, it was successfully activated for 70 minutes and used in PDMS@PDMS bonding. BERDICHEVSKY et al. [31] described the formation of cracks at high temperatures and ascribed it to the hardened surface and an up to 30% shrinkage of the treated layer. This shrinkage value is most likely different in our case, as it depends on the lamp intensity which is not given. However, this suggests that the combination of the membrane's high flexibility and its hardening due to ozone exposure results in micro-cracks forming on the surface. The increase in surface roughness could then cause the weak bonding.

Furthermore, reverse bonding of the membrane was tested as a workaround. For this, a spin-coated glass substrate was bonded to a PDMS microfluidic layer using the 70-minute ozone treatment. The 0.11 mm-thick membrane was then carefully peeled off the glass substrate. It was damaged when reaching a 1.5 mm diameter cut-out in the PDMS layer, most likely due to a combination of high mechanical stress and the slight hardening of the membrane. For this study, we concluded that microfluidic chips should be prepared using spin-coated glass or PDMS substrates, and PDMS membranes should be avoided.

3.2. Decrease the Mechanical Stress Within the PDMS Surrounding the Inlets

Punctual pressure comes with a risk of crack formation in the surface and the PDMS@PDMS bonding strength is also weaker in comparison to activation with the oxygen plasma treatment [31,32]. This was observable when we did first tests to prepare microfluidic chips with the 70 min UVO treatment time (see SI Figure S2). In order to minimize the impact of these cracks and weak bonding, microfluidic chips with the predetermined breaking structures surrounding the inlet were prepared using photolithography and soft lithography processes. Cracks still appeared in the bonded surfaces when a 1 mm or 1.6 mm tube was inserted into an inlet created with a 1 mm or 1.5 mm biopsy punch, respectively (see SI, Figure S4). This is because the PDMS bends during punching, creating a hole with a smaller diameter than that of the puncher used. When the tube is inserted, the resulting strain within the PDMS leads to cracks in the surface.

Further mechanical stability tests on the structures were therefore performed by adding a 1 mm tube to a 1.5 mm inlet. Depending on how much the PDMS bends during punching, this either fits exactly or is slightly too small, leaving a small gap between tube and PDMS wall. Each structure was prepared four times. Examples of the micrographs are given in Figure 6 and all pictures are compiled in the SI Table S2. The tubes were moved and pressed to mimic the careful handling of a microfluidic chip during laboratory testing. As observable in Figure 6 2A-2E, this results in small cracks or punctual breaking of the bonding (as indicated by the lighter-colored spots), but the structures could still be used even without the predetermined breaking cycles.

However, long-term use or careless handling could result in elongation of the cracks. Therefore, the PDMS around the tubes was deliberately damaged by pressing and moving them with greater force in order to identify their weak spots. Some of the resulting images are shown in Figure 6 3A-3E. According to these images, discontinuous circular structures around the inlets and outlets prevent detachment in the event of a weak bonding. However, the interrupted ring area is vulnerable to cracking. Uniform rings around the inlets and outlets prevent further detachment in the event of weak bonding, while also sufficiently interrupting cracks. Two ring structures protect the best, but they also need more space, so depending on the microfluidic device one ring structure might be more sufficient in some cases. This will extend the lifetime of the microfluidic chip during handling in a laboratory setting, for example when tubes are repeatedly connected to other devices or when a chip is accidentally dropped.

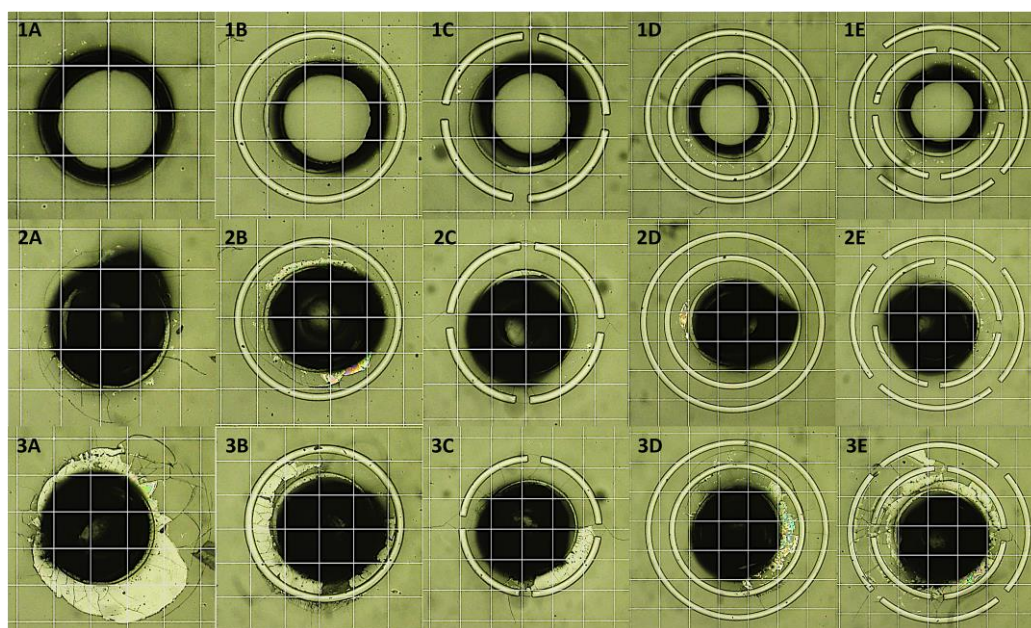


Figure 6. Micrographs of 1.5 mm inlets with different predetermined breaking structures (A-E) before inserting a tube (1) and after inserting 1 mm tubes and moving them to mimic usual handling of a microfluidic device (2) and after moving and pressing with extended force to purposefully damage the structures (3). The test was performed with four different chips and the presented pictures are examples. All pictures are given in SI Table S1 For all pictures the contrast and sharpness were increased for better visualization of the damages. A square equals 500 μm x 500 μm .

The main problem when using biopsy punches that are larger than the tubes, is ensuring that the inlets and outlets are properly sealed without blocking the channels when the tubes are glued with pre-polymerized PDMS. As solution different PDMS seals were prepared. The seals with 2 mm outer diameter were not tested further as they were difficult to handle and easily damaged. Moreover, the 0.1 mm and 0.2 mm thick seals were difficult to handle as they bent easily, allowing glue to enter the space between the tube and the wall. Additionally, when an outer diameter of 5 mm was used, the tubes could easily be pulled out after the glue had cured, resulting in a lack of mechanical stability. For the 1 mm and 1.5 mm tubes, seals of 3-4 mm outer diameter and 0.5 mm thickness were the easiest to use. In some cases, the seals did not fully prevent the PDMS from entering the space between tube and wall, but it was getting in so slowly that the channels were not clogged as observable in SI Figure S5. We found that using pre-polymerized PDMS glue to seal microfluidic chips is helpful when bonding or leakage problems occur. The viscosity of freshly prepared PDMS is usually too low to prevent it from entering very small gaps before it is fully cured. With pre-polymerized PDMS, however, this risk is much lower and the glue is applied easily with a spatula when it has a honey-like consistency. Using a stand to stabilize the tube positions while gluing, with the chip already placed on hotplates, would greatly improve this process. However, compared to oxygen plasma-treated samples, where the punched holes can be smaller than the tubes' outer diameter and the PDMS seals the tubes without glue, this process is more susceptible to errors.

3.3. Functionality of Microfluidic Chips Prepared Using UVO Bonding

With this knowledge, two microfluidic chips were prepared (Figure 7) to serve as a proof that functional microfluidic chips **MF1** and **MF2** can be realized when using a UVO treatment. In this case, no predetermined breaking structures were used since the chips were not intended for long-term use. The gluing of the tubes was found to be sensitive to manual handling errors. For example, in case of **MF1** the bottom left tube fell to the site while gluing the middle tube and the glue clogged the corresponding inlet. To prevent this problem, a stand will be used in the future.

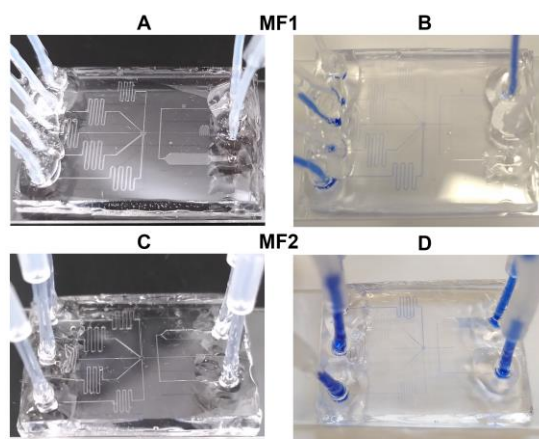


Figure 7. Photographs of the microfluidic chips **MF1** and **MF2**: on the left, after the tubes have been glued on; on the right, in use with blue ink. In case of **MF1** (A and B), the bottom left tube has fallen off during gluing, and the inlet has become clogged with glue, rendering it unusable.

The chips were used in a leakage test involving blue-ink-colored water. There were no internal bridges between channels observable, which would indicate poor bonding due to insufficient activation of the surface. The pressure measurement for the chip **MF1** is shown in Figure 8 and the measurement for **MF2** is given in the SI in Figure S6. Both chips could be used in vacuum and pressure-driven systems, when they were connected to a stepper pump capable of generating a flow of $170 \mu\text{L}/\text{min}$ and applying a pressure of at least $\pm 180 \text{ mbar}$. The tubes were then closed with fold back clamps for the burst test. The pressure increased up to a point when a leakage appeared to determine the maximum possible pressure. In both cases, leakage occurred at around 500 mbar . At this point, bonding broke across a wider area of the two layers, as observable in the photographs provided in SI Figure S7. This is lower than for microfluidic chips prepared using oxygen plasma bonding which we were able to operate up to at least 900 mbar . This is consistent with the weaker bonding strength described by YOUSUFF et al. [32]. Nevertheless, this range is suitable for typical laboratory tests.

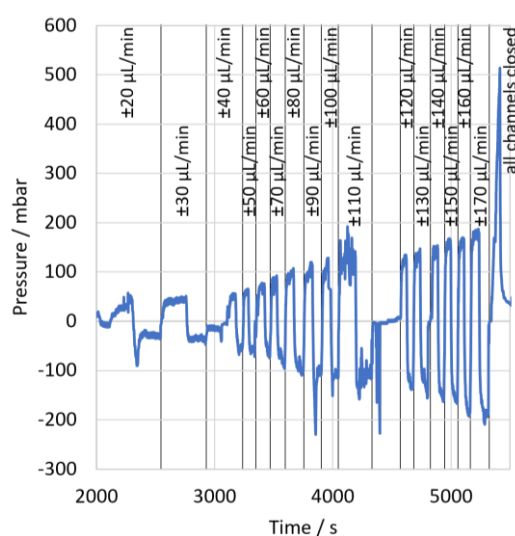


Figure 8. Results of the pressure measurement as a function of time and the different flow values used to proof functionality and leak test as well as burst test (starting at $\sim 5200 \text{ s}$) of **MF1**.

4. Conclusions

In conclusion, we presented a protocol for preparing microfluidic chips that uses the UV ozone cleaner by Ossila for bonding instead of oxygen plasma bonding. The process is limited to PDMS@PDMS bonding and problems caused by the hardening of the surface were overcome. Although this process is slower in comparison to oxygen plasma bonding, it is carried out using a less expensive, easier-to-handle instrument. This can be a viable alternative when only small quantities of microfluidic chips are required and an oxygen plasma etcher is unavailable. In order to gain a broader understanding of UVO bonding in general, it would be interesting to compare the bonding processes, geometries and lamp intensities of different instruments, in order to determine the most effective instrument and bonding conditions. However, this cannot be achieved using the limited information available in the existing literature.

5. Patents

The authors declare that the predetermined braking structures and sealing process of the tubes have been filed for patent under the number (DE10 2026 109 856).

Supplementary Materials: The following supporting information can be downloaded at the website of this paper posted on Preprints.org, Table S 1: Overview on the different conditions described in literature for UVO bonding. n.p. = not provided (there is no guarantee of completeness); Figure S 1: Photograph of the UV Ozone cleaner by Ossila; Figure S 2: Pictures of cracks at the bonded surfaces of a microfluidic chips when applying punctual pressure; Figure S 3: Design of the inlets with predetermined braking structures; Figure S 4: Top: Inlets with surrounding predetermined braking structures before (top) and after inserting tubes (bottom). In case A the hole was prepared with a 1 mm biopsy punch and the tube has 1 mm OD. In case of B, C and D the hole was punched with a 1.5 mm puncher and the tube has an OD of 1.6 mm. For all pictures contrast and sharpness were increased to increase the visibility of the fine cracks; Table S 1: Micrographs from the mechanical stability test. Each structure was prepared and tested four times. For all pictures contrast and sharpness were increased to increase the visibility of the fine cracks; Figure S 5: Example on how to seal a tube of 1.6 mm outer diameter (OD) to an inlet created with a 2 mm biopsy punch by using a seal with inner diameter (ID) of 1.5 mm and OD of 4 mm; Figure S 6: Left: Examples of micrographs of tubes glued with pre-polymerized PDMS (in this case colored with carbon black to make the PDMS glue and the seals easier visible). In all cases, the PDMS glue got between the wall and the tube, but did not reach the end of the tube. Even though the PDMS was colored with carbon black, it is difficult to see the glue, which is why manual handling of the seals was chosen as an exclusion criterion instead of the most effective way of preventing PDMS from getting in; Figure S 7: Results of the pressure measurement as a function of time and the different flow values used to proof functionality of MF2. The larger scattering in comparison to the results for MF1 is due to air bubbles in the tubes and the MF chip; Figure S 8: MF1 (left) and MF2 (right) after the burst test. In both cases the leakage (left) and the area where the bonding was broken due to the high pressure (coloured with blue ink) can be seen (right).

Author Contributions: Conceptualization, M.P., M.G.; methodology, M.P.; software, L.H., and I.T.; validation, M.P.; formal analysis, M.P., L.H., I.T.; investigation, M.P.; resources, M.P.; data curation, L.H. and I.T.; writing—original draft preparation, M.P.; writing—review and editing, M.P., L.H., I.T., and M.G.; visualization, M.P.; supervision, M.G.; project administration, M.G.; funding acquisition, M.G. All authors have read and agreed to the published version of the manuscript.

Funding: Funded by the European Union. Views and opinions expressed are however those of the authors only and do not necessarily reflect those of the European Union or the European Research Council Executive Agency. Neither the European Union nor the granting authority can be held responsible for them. This work is supported by EIC Transition grant SOILMONITOR, 101097989.

Data Availability Statement: The data supporting this article and the DWG-files of the structures have been included as part of the Supplementary Information.

Acknowledgments: The authors thank Natali Alhijazeen and Paul Koch for contributing to the resources by preparing the PDMS samples and Jannika Rolfs and Ali Allouch for contributing ideas to the tests and microfluidic structure, respectively.

Conflicts of Interest: Aside from the patent mentioned above, there are no further competing interests to declare.

Abbreviations

The following abbreviations are used in this manuscript:

PDMS	Polydimethylsiloxane
UVO	UV Ozone
MF	Microfluidic chip
PGMEA	1-Methoxy-2-propylacetat

References

1. Noviana, E.; Ozer, T.; Carrell, C.S.; Link, J.S.; McMahon, C.; Jang, I.; Henry, C.S. Microfluidic Paper-Based Analytical Devices: From Design to Applications. *Chem. Rev.* **2021**, *121*, 11835–11885, doi:10.1021/acs.chemrev.0c01335.
2. Nge, P.N.; Rogers, C.I.; Woolley, A.T. Advances in Microfluidic Materials, Functions, Integration, and Applications. *Chem. Rev.* **2013**, *113*, 2550–2583, doi:10.1021/cr300337x.
3. Gharib, G.; Bütün, İ.; Muganlı, Z.; Kozalak, G.; Namlı, İ.; Sarraf, S.S.; Ahmadi, V.E.; Toyran, E.; Van Wijnen, A.J.; Koşar, A. Biomedical Applications of Microfluidic Devices: A Review. *Biosensors* **2022**, *12*, 1023, doi:10.3390/bios12111023.
4. Fallahi, H.; Zhang, J.; Phan, H.-P.; Nguyen, N.-T. Flexible Microfluidics: Fundamentals, Recent Developments, and Applications. *Micromachines* **2019**, *10*, 830, doi:10.3390/mi10120830.
5. Sun, K.; Fan, Y.; Hebda, M.; Zhang, Y. Origami Microfluidics: A Review of Research Progress and Biomedical Applications. *Biomed. Mater. Devices* **2023**, *1*, 388–401, doi:10.1007/s44174-022-00007-2.
6. Haerberle, S.; Zengerle, R. Microfluidic Platforms for Lab-on-a-Chip Applications. *Lab Chip* **2007**, *7*, 1094, doi:10.1039/b706364b.
7. Auroux, P.-A.; Iossifidis, D.; Reyes, D.R.; Manz, A. Micro Total Analysis Systems. 2. Analytical Standard Operations and Applications. *Anal. Chem.* **2002**, *74*, 2637–2652, doi:10.1021/ac020239t.
8. Qamar, A.Z.; Shamsi, M.H. Desktop Fabrication of Lab-On-Chip Devices on Flexible Substrates: A Brief Review. *Micromachines* **2020**, *11*, 126, doi:10.3390/mi11020126.
9. Kraft, F.A.; Schardt, J.; Kitzler, D.; Latz, A.; Gerken, M. Exfoliated Flexible Photonic Crystal Slabs for Refractive Index and Biomolecular Sensing. *IEEE Flex. Electron.* **2023**, *2*, 136–144, doi:10.1109/JFLEX.2023.3234894.
10. Gao, Y.; Wu, M.; Lin, Y.; Xu, J. Acoustic Microfluidic Separation Techniques and Bioapplications: A Review. *Micromachines* **2020**, *11*, 921, doi:10.3390/mi11100921.
11. Lei, K.F. Microfluidic Systems for Diagnostic Applications: A Review. *J Lab Autom.* **2012**, *17*, 330–347, doi:10.1177/2211068212454853.
12. Lim, Y.C.; Kouzani, A.Z.; Duan, W. Lab-on-a-Chip: A Component View. *Microsyst Technol* **2010**, *16*, 1995–2015, doi:10.1007/s00542-010-1141-6.
13. Niculescu, A.-G.; Chircov, C.; Bîrcă, A.C.; Grumezescu, A.M. Fabrication and Applications of Microfluidic Devices: A Review. *Int. J. Mol. Sci* **2021**, *22*, 2011, doi:10.3390/ijms22042011.
14. Scott, S.; Ali, Z. Fabrication Methods for Microfluidic Devices: An Overview. *Micromachines* **2021**, *12*, 319, doi:10.3390/mi12030319.
15. Sathyanarayanan, G.; Haapala, M.; Dixon, C.; Wheeler, A.R.; Sikanen, T.M. A Digital-to-Channel Microfluidic Interface via Inkjet Printing of Silver and UV Curing of Thiol-Enes. *Adv. Materials Technologies* **2020**, *5*, 2000451, doi:10.1002/admt.202000451.
16. Giri, K.; Tsao, C.-W. Recent Advances in Thermoplastic Microfluidic Bonding. *Micromachines* **2022**, *13*, 486, doi:10.3390/mi13030486.

17. Zhang, Y.; Sun, K.; Xie, Y.; Liang, K.; Zhang, J.; Fan, Y. Reversible Bonding of Microfluidics: Review and Applications. *Rev. Sci. Instrum.* **2023**, *94*, 061501, doi:10.1063/5.0142551.
18. Sivakumar, R.; Lee, N.Y. Microfluidic Device Fabrication Mediated by Surface Chemical Bonding. *Analyst* **2020**, *145*, 4096–4110, doi:10.1039/D0AN00614A.
19. Raj M, K.; Chakraborty, S. PDMS Microfluidics: A Mini Review. *J. Appl. Polym. Sci* **2020**, *137*, 48958, doi:10.1002/app.48958.
20. Akbari, Z.; Raoufi, M.A.; Mirjalali, S.; Aghajanloo, B. A Review on Inertial Microfluidic Fabrication Methods. *Biomicrofluidics* **2023**, *17*, 051504, doi:10.1063/5.0163970.
21. Walsh, D.I.; Kong, D.S.; Murthy, S.K.; Carr, P.A. Enabling Microfluidics: From Clean Rooms to Makerspaces. *Trends Biotechnol.* **2017**, *35*, 383–392, doi:10.1016/j.tibtech.2017.01.001.
22. McDonald, J.C.; Duffy, D.C.; Anderson, J.R.; Chiu, D.T.; Wu, H.; Schueller, O.J.A.; Whitesides, G.M. Fabrication of Microfluidic Systems in Poly(Dimethylsiloxane). *Electrophoresis* **2000**, *21*, 27–40, doi:10.1002/(SICI)1522-2683(20000101)21:1%3C27::AID-ELPS27%3E3.0.CO;2-C.
23. Borók, A.; Laboda, K.; Bonyár, A. PDMS Bonding Technologies for Microfluidic Applications: A Review. *Biosensors* **2021**, *11*, 292, doi:10.3390/bios11080292.
24. Eddings, M.A.; Johnson, M.A.; Gale, B.K. Determining the Optimal PDMS–PDMS Bonding Technique for Microfluidic Devices. *J. Micromech. Microeng.* **2008**, *18*, 067001, doi:10.1088/0960-1317/18/6/067001.
25. Douville, N.J.; Tung, Y.-C.; Li, R.; Wang, J.D.; El-Sayed, M.E.H.; Takayama, S. Fabrication of Two-Layered Channel System with Embedded Electrodes to Measure Resistance Across Epithelial and Endothelial Barriers. *Anal. Chem.* **2010**, *82*, 2505–2511, doi:10.1021/ac9029345.
26. Man Lung Sham; Jing Li; Peng Cheng Ma; Kim, J.-K. Cleaning and Functionalization of Polymer Surfaces and Nanoscale Carbon Fillers by UV/Ozone Treatment: A Review. *J. Compos. Mater.* **2009**, *43*, 1537–1564, doi:10.1177/0021998308337740.
27. Jakubowsky, M.; Werder, J.; Rytka, C.; Kristiansen, P.M.; Neyer, A. Design, Manufacturing and Experimental Validation of a Bonded Dual-Component Microstructured System for Vertical Light Emission. *Microsyst Technol* **2020**, *26*, 2087–2093, doi:10.1007/s00542-020-04767-z.
28. Tsao, C.W.; Hromada, L.; Liu, J.; Kumar, P.; DeVoe, D.L. Low Temperature Bonding of PMMA and COC Microfluidic Substrates Using UV/Ozone Surface Treatment. *Lab Chip* **2007**, *7*, 499–505, doi:10.1039/B618901F.
29. Bhattacharyya, A.; Klapperich, C.M. Mechanical and Chemical Analysis of Plasma and Ultraviolet–Ozone Surface Treatments for Thermal Bonding of Polymeric Microfluidic Devices. *Lab Chip* **2007**, *7*, 876–882, doi:10.1039/B700442G.
30. Efimenko, K.; Wallace, W.E.; Genzer, J. Surface Modification of Sylgard-184 Poly(Dimethyl Siloxane) Networks by Ultraviolet and Ultraviolet/Ozone Treatment. *J. Colloid. Interface Sci.* **2002**, *254*, 306–315, doi:10.1006/jcis.2002.8594.
31. Berdichevsky, Y.; Khandurina, J.; Guttman, A.; Lo, Y.-H. UV/Ozone Modification of Poly(Dimethylsiloxane) Microfluidic Channels. *Sens. Actuators B: Chem.* **2004**, *97*, 402–408, doi:10.1016/j.snb.2003.09.022.
32. Yousuff, C.M.; Danish, M.; Ho, E.T.W.; Kamal Basha, I.H.; Hamid, N.H.B. Study on the Optimum Cutting Parameters of an Aluminum Mold for Effective Bonding Strength of a PDMS Microfluidic Device. *Micromachines* **2017**, *8*, 258, doi:10.3390/mi8080258.
33. Chen, H.-Y.; McClelland, A.A.; Chen, Z.; Lahann, J. Solventless Adhesive Bonding Using Reactive Polymer Coatings. *Anal. Chem.* **2008**, *80*, 4119–4124, doi:10.1021/ac800341m.
34. Holtorf, L.; Poschmann, M.; Titov, I.; Gerken, M. A Miniaturized Lab-on-Chip System for the Measurement of Nitrate in Water. In Proceedings of the 2025 IEEE Sensors Applications Symposium (SAS); July 2025; pp. 1–5.

Disclaimer/Publisher’s Note: The statements, opinions and data contained in all publications are solely those of the individual author(s) and contributor(s) and not of MDPI and/or the editor(s). MDPI and/or the editor(s) disclaim responsibility for any injury to people or property resulting from any ideas, methods, instructions or products referred to in the content.